RAA 2021 Vol. **21** No. **9**, 240(7pp) doi: 10.1088/1674-4527/21/9/240

http://www.raa-journal.org *http://iopscience.iop.org/raa*

***R**esearch in*
***A**stronomy and*
***A**strophysics*

A single pulse study of PSR J1752+2359

Sheng-Nan Sun (孙盛楠)[1,2], Wen-Ming Yan (闫文明)[1,3,4], Na Wang (王娜)[1,3,4] and Rai Yuen[1,3]

[1] Xinjiang Astronomical Observatory, Chinese Academy of Sciences, Urumqi 830011, China; *yanwm@xao.ac.cn; na.wang@xao.ac.cn*
[2] University of Chinese Academy of Sciences, Beijing 100049, China
[3] Key Laboratory of Radio Astronomy, Chinese Academy of Sciences, Nanjing 210008, China
[4] Xinjiang Key Laboratory of Radio Astrophysics, 150 Science1-Street, Urumqi 830011, China

Received 2021 April 17; accepted 2021 June 7

Abstract The single pulse observation of PSR J1752+2359 at 1250 MHz made using the Five-hundred-meter Aperture Spherical radio Telescope (FAST) is presented. We show that the pulsar exhibits two distinct emission states: a normal state with continuous normal pulse emission and a rotating radio transient (RRAT)-like state with sporadic emission. This makes PSR J1752+2359 the third pulsar that exhibits switching between RRAT-like and pulsar-like states. Our data show that, during the observation, 20 per cent of the time for this pulsar was in the normal state and 80 per cent in the RRAT-like state. A quasi-periodic switching, with a periodicity of around 568 spin periods, between the two states was observed. The pulse energies for the two states both follow log-normal distributions. We demonstrate that the polarization profiles and the linear polarization position angle (PA) swings differ significantly between the two states. There is a phase offset of about $0^{\circ}.35$ between the pulse profile peaks of the two states. We argue that the emission geometry in the magnetosphere may be different for the two states.

Key words: stars: neutron — pulsars: general — pulsars: individual (PSR J1752+2359)

1 INTRODUCTION

Pulsars, discovered by Jocelyn Bell and Antony Hewish in 1967 (Hewish et al. 1968), are rapidly rotating and highly magnetized neutron stars, which have been observed to show various emission properties across wide frequency bands, such as in the radio, optical, X-ray and Gamma ray (Lyne & Graham-Smith 2012; Lorimer & Kramer 2012). Pulsar nulling was discovered by Backer (1970), and subsequent studies of the null duration in different pulsars show that the value lies in the range of several spin periods to many hours or even days (Wang et al. 2007). The "nulling fraction" (NF), the total fraction of time during which the pulsar is in a null state, can vary from close to zero to over 90% (Biggs 1992; Wang et al. 2007). Early studies suggested that the NF was related to the pulsar age, and that older pulsars tended to have a higher fraction of null pulses (Ritchings 1976). Other investigations found that the NF showed better correlation with spin period (Biggs 1992; Wang et al. 2020a). The intermittent pulsars may be considered as an extreme form of nulling, where the pulse emission vanishes from several days to years (Kramer et al. 2006; Wang et al. 2020b). Mode changing is another emission phenomenon, in which the average pulse profile of a pulsar abruptly changes between two or more stable states (Bartel et al. 1982). Pulsar nulling and mode changing are suggested as different manifestations of the same phenomenon (Wang et al. 2007).

Rotating radio transients (RRATs) are an unusual class of pulsars. The first RRAT was discovered in the archival data from the Parkes multi-beam pulsar survey (McLaughlin et al. 2006). Emission from RRATs exhibits as sporadic bursts that occur at intervals between few minutes to hours. The typical duration of a burst is about several milliseconds. The total number of RRATs currently known is 112[1]. Their spin periods and period derivatives range from 0.125 to 7.707 s and from 0.29×10^{-15} to $5.75 \times 10^{-13}\,\mathrm{s\,s^{-1}}$, respectively. RRATs tend to have higher surface magnetic field compared to normal pulsars (Harding 2013). Like normal pulsars, the pulse energies for most RRATs follow log-normal distributions (Cui et al. 2017). To date, the emission mechanism of RRATs is still unclear. However, Burke-Spolaor & Bailes (2010) found that PSR J0941−39 oscillates between an RRAT and a pulsar, which provides a link between pulsars and RRATs.

[1] http://astro.phys.wvu.edu/rratalog/

PSR B0826−34 is the second pulsar that shows such behavior (Esamdin et al. 2012).

PSR J1752+2359 was discovered in the high galactic latitude pulsar survey of the Arecibo sky, which has a spin period of 0.409 s (Foster et al. 1995). An early study of the pulsar at 430 MHz by Lewandowski et al. (2004) showed that it exhibits bursting emission similar to PSRs J1938+2213 (Lorimer et al. 2013) and B0611+22 (Seymour et al. 2014). Using the Giant Meterwave Radio Telescope and the 305-m Arecibo Telescope, Gajjar et al. (2014) found that the burst emission from the pulsar exhibits quasi-periodic pattern. They also noticed that, during the null state, PSR J1752+2359 shows some isolated burst emissions whose integrated pulse profile is different from that of the burst state. This phenomenon is reminiscent of an RRAT. However, they did not give more details about these isolated bursts.

In this paper, we continue the earlier work of Gajjar et al. (2014) on PSR J1752+2359 by using the Five-hundred-meter Aperture Spherical radio Telescope (FAST) (Nan 2008; Nan et al. 2011) observations. With high sensitivity, FAST is an ideal tool to study pulsar single pulses (e.g., Zhang et al. 2019; Feng et al. 2021; Wang et al. 2021). Our highly sensitive observation provides an opportunity to study the isolated bursts in the null state of PSR J1752+2359. In Section 2, we describe the observation and data processing, and the results are presented in Section 3. In Section 4, we discuss and summarize our results.

2 OBSERVATIONS

Being the world's largest single-aperture radio telescope, FAST has a maximum effective aperture of 300 m in diameter and has been operating since September 2016. The 19-beam L-band receiver that covers 1.05–1.45 GHz was installed in May 2018 (Li et al. 2018; Jiang et al. 2019). Our observation was performed on 2020 August 26 using the center beam of the 19-beam receiver at 1250 MHz center frequency. The total observation time was about 1.5 hours and 13 057 single pulses were obtained in total. The data were recorded using the search mode of the PSRFITS data format (Hotan et al. 2004) with a sampling time of 49.152 μs and 4096 frequency channels.

For the data analysis, we used DSPSR (van Straten & Bailes 2011) to extract individual pulses based on the ephemeris provided by PSRCAT (Manchester et al. 2005). Then we used the PAZ and PAZI plugins in the PSRCHIVE package (Hotan et al. 2004) to remove the 5% of the band-edges and flag narrow-band and impulsive radio-frequency interference (RFI) in the data, respectively. For the polarization calibration, we folded the calibration files with a period of 0.201326592 s and then calibrated the pulsar data to obtain the Stokes parameters (Wang et al. 2020c) using PAC in the PSRCHIVE program. We fitted the rotation measure (RM) using the RMFIT program of the PSRCHIVE package and obtained 89.5 ± 0.6 rad m^{-2}, which is consistent with the value of 87.05 ± 0.11 rad m^{-2} given by Sobey et al. (2019).

Table 1 Polarization Parameters for the Normal and the RRAT-like States

State	$\langle L\rangle$/S (%)	$\langle V\rangle$/S (%)	$\langle\|V\|\rangle$/S (%)	W50 (°)
Normal state	27.59	–1.31	4.73	5.10
RRAT-like state	43.85	–2.80	9.11	1.89

3 THE RESULTS

3.1 The Two Emission States

The pulse stack of the 13 057 single pulses of PSR J1752+2359 in our observation is shown in Figure 1. The emission from this pulsar demonstrates two different states: the normal state with continuous pulse emission (labeled by the white rectangles in Fig. 1) and the RRAT-like state with sporadic pulse emission. A normal state was determined by eyes, and 30 such states (pulse blocks) in total of 2581 single pulses were identified. In the RRAT-like state, the pulsar behaves as if pulse nulling superposed with sporadic and bright pulses. An example of emission in the RRAT-like state is shown in the rightmost panel in Figure 1. Variation in the peak flux intensity, normalized to the peak flux intensity of the mean pulse profile, for a sequence of 995 single pulses is shown in Figure 2. The sporadic pulses in the RRAT-like state are indicated by the red arrows in the figure. We estimate that the pulsar spends 20 per cent of time in the normal state and 80 per cent in the RRAT-like state in our observation.

The pulse energy distributions for the normal state, RRAT-like state, and for the off-pulse window are shown in Figure 3. For each single pulse, the pulse energy was calculated by summing the intensities within the on-pulse window, whose width is determined by the average pulse profile, after subtracting the baseline noise. The off-pulse energy was estimated using the same method with an off-pulse window of the same duration as the on-pulse window. The pulse energy for the normal state follows a log-normal distribution as shown by the red dashed line. The energy distribution of the RRAT-like state can be fitted by a Gaussian function (the blue dashed line) that peaks at zero with a high-energy tail that corresponds to the sporadic pulses. The distribution for the off-pulse energy is in good agreement with a normal distribution that peaks at zero.

To investigate the energy distribution of the sporadic pulses in the RRAT-like state, we selected pulses with the signal-to-noise ratio (S/N) larger than six, and 130 such

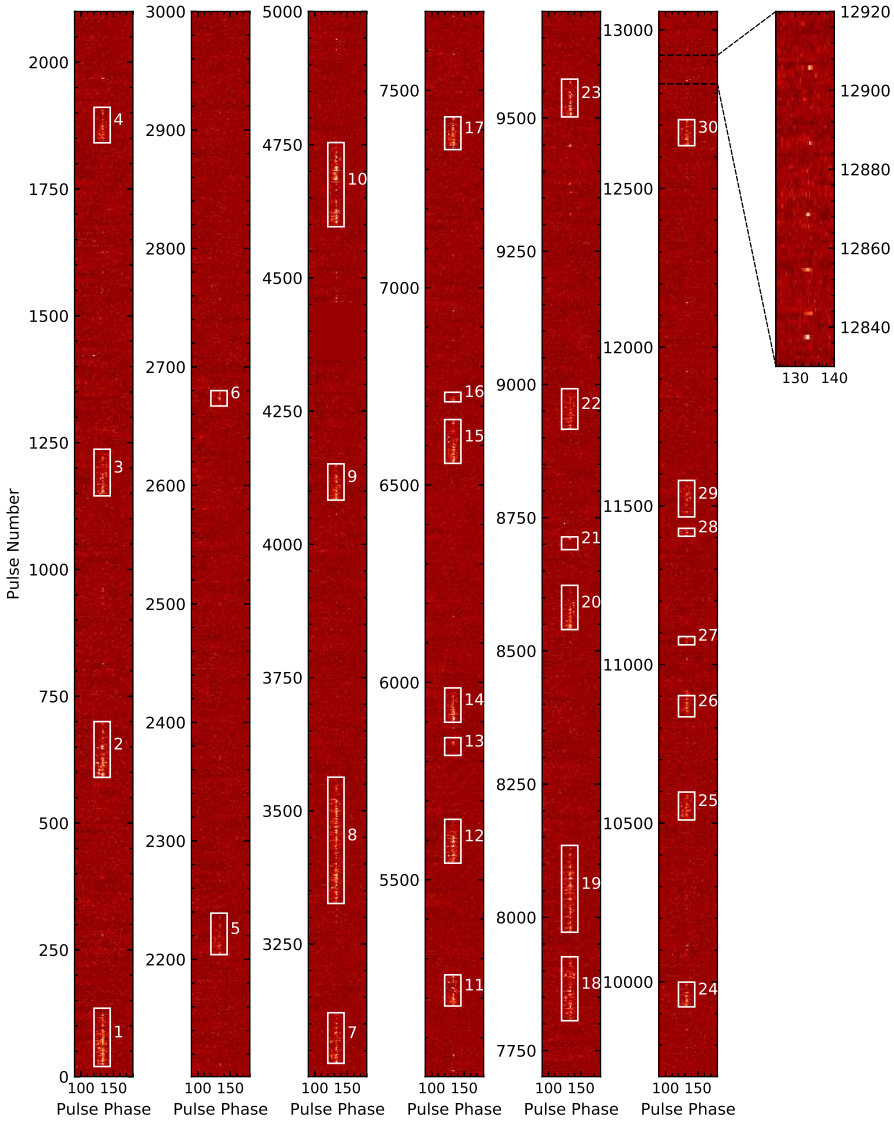

Fig. 1 The 13 057 individual pulses observed in PSR J1752+2359. Thirty normal pulse emission states are identified, which are indicated by the *white rectangles*. A zoom-in view is presented in the rightmost panel showing several bright pulses in the RRAT-like state. Pulses 4342−4446 have been removed due to the strong interference.

pulses were obtained. The S/N was calculated as the ratio between the peak intensity within the on-pulse window and the root-mean-square (rms) of the baseline. As indicated by the green dashed line in the inset plot in Figure 3, the energy distribution of the sporadic pulses can be fitted by a log-normal function, which is a typical feature for most RRATs (see Cui et al. 2017).

The polarization properties of the normal state and the RRAT-like state are shown in Figure 4 for comparison. The average pulse profile of the normal state in our observation has three components, which is consistent with previous results obtained at 430 MHz (Gajjar et al. 2014). The sporadic pulses in the RRAT-like state have pulse widths that are much narrower than that in the normal state, and they are found within a narrow pulse phase range. We also found that the offset of the profile peaks between the two states is about $0.^{\circ}35$ at 1250 MHz which is slightly smaller than that of $0.^{\circ}6$ at 327 MHz (Gajjar et al. 2014).

Table 1 shows a summary of the polarization parameters for the average pulse profiles of the two states, which includes the mean linear polarization intensity $\langle L \rangle$, the mean circular polarization intensity $\langle V \rangle$, the mean absolute circular polarization intensity $\langle |V| \rangle$ and the full width at half maximum (W50). The peak flux intensity of the average profile in the RRAT-like state is about 1.4 times larger than that of the normal state. For the normal state, the linear polarization and circular polarization intensities for both the first and third components are weak. The fractional linear polarization intensities in the central component are relatively strong in both states. Figure 5

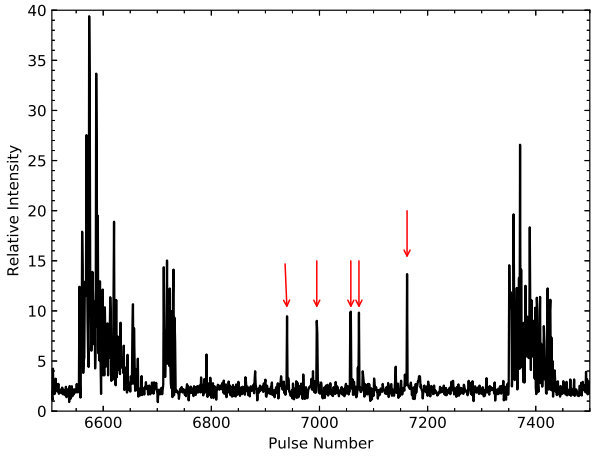

Fig. 2 Variation in the normalized peak flux intensity for 995 successive pulses of J1752+2359. The *red arrows* signify strong sporadic pulses, each with S/N greater than six, in the RRAT-like state.

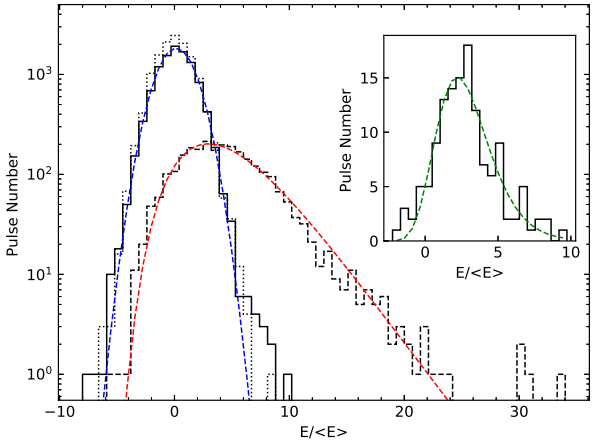

Fig. 3 Pulse energy distributions for the off-pulse region (*dotted histogram*) and the on-pulse region, where the latter is separated into the RRAT-like state (*solid histogram*) and the normal state (*dashed histogram*). The energy distribution of the 130 sporadic strong pulses, each with S/N greater than six in the RRAT-like state, is shown in the inset plot. The energies are normalized by the mean on-pulse energy. The *blue*, *red* and *green dashed lines* represent the lines of best fit for the RRAT-like state, normal state and the sporadic pulses, respectively.

shows the position angle (PA) swings in the normal (black dots) and the RRAT-like (red dots) states. It is clear that the PA variations in the two states are different. Therefore, we suggest that the geometry of the magnetospheric field is different in the two states.

We derive the mean pulse profiles for the first and last ten detectable pulses for all pulse blocks in the normal state, respectively. Note that blocks with pulse numbers less than 20 are excluded. The average profiles for the first ten pulses (FP) and the last ten pulses (LP) in the normal state are shown in Figure 6. For the average profile of the FP, the linear polarization intensity is weak for the first and the third components, while it is relatively high in the second component. This is similar to the average profile obtained from all pulses in the normal state. In addition, the PA variation of the FP is also similar to that of the normal state. On the contrary, the average profile of the LP has only one weak main component which is related to the central component of the FP. The PA swing of the LP is also coincident with that of the average profile of the normal state. Our results suggest that the first and third pulse components disappear prior to the second pulse component towards the end of the normal state, while all three components are present at the beginning of the normal state. The peak flux intensity of FP is the same as that of the average profile in the normal state. However, the peak flux intensity of FP is much stronger (about 2.7 times) than that of LP. This implies that the pulse energy decreases with time during the normal state, which is in agreement with the results of Lewandowski et al. (2004) and Gajjar et al. (2014).

Figure 7 shows the distribution histograms of pulse peak flux intensity for the RRAT-like and the normal states in panels (a1) and (a2), respectively. Note that only single pulses with S/N greater than six from both states are included. The peak flux intensity of the RRAT-like state is in the range of 5 to 20, whereas the normal state has a much wider distribution with the range covering between 5 and 60. We calculate the pulse width by fitting the pulses in the RRAT-like state and the central component of the pulses in the normal state with Gaussian functions. The resulted half-power pulse widths W50 are presented in Figure 7. The pulses in the RRAT-like state are narrow, typically less than 7 ms, whereas those in the normal state are widely distributed with the widest W50 reaching about 33 ms. The normal state also shows some narrow single pulses whose widths are similar to the pulses in the RRAT-like state.

3.2 Periodicity

Periodic mode changing or nulling has been seen in many pulsars, such as PSRs B1133+16 (Herfindal & Rankin 2007), J1819+1305 (Rankin & Wright 2008), J1825−0935 (Yan et al. 2019) and J1048−5832 (Yan et al. 2020). It is known that the occurrence of the normal state for PSR J1752+2359 is also periodic. Using the Giant Meterwave Radio Telescope, Gajjar et al. (2014) analyzed the periodicity of the occurrence of the normal state with a one-dimensional pair correlation function. They found that the normal state of PSR J1752+2359 occurred in a quasi-periodic fashion at 325 MHz with three periodic features at 540, 595 and 490 pulses. To confirm the existence of the periodicity for this pulsar at a higher observing frequency, we perform an analysis of fluctuation spectrum

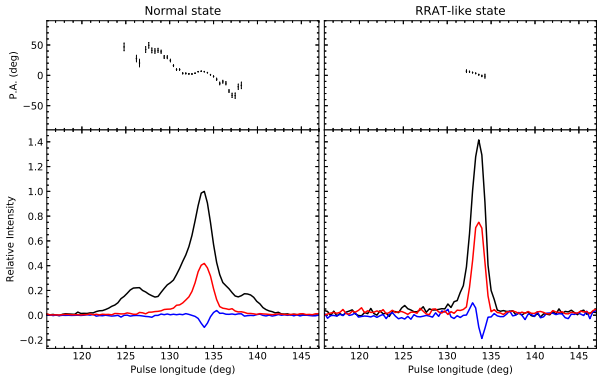

Fig. 4 Polarization profiles for the normal state (*left*) and the RRAT-like state (*right*). The *black*, *red* and *blue lines* represent the total, linear polarization and circular polarization intensities, respectively. The *black dots* with error bars in the two upper panels indicate the PA of the linear polarization.

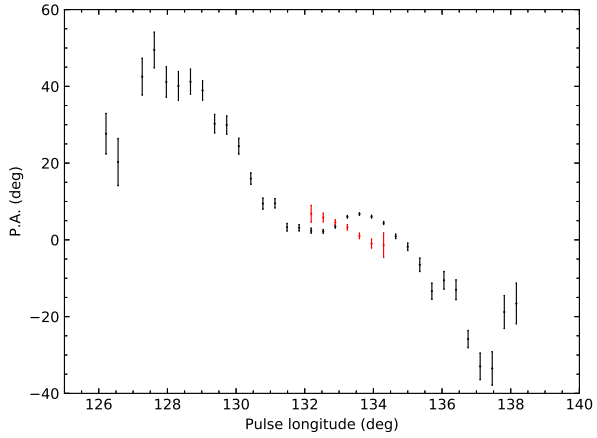

Fig. 5 Changes in the PAs of the linear polarization in the normal (*black dots*) and RRAT-like (*red dots*) states.

based on fast Fourier transform (FFT) for determining the modulation period (Gajjar et al. 2017). We set the pulses in the normal state as 'one' and that in the RRAT-like state as 'zero'. The resulting fluctuation spectrum is shown in Figure 8, in which a quasi-periodic feature of 568 pulse periods (232 s) is detected. The value is consistent with the results given by Gajjar et al. (2014).

4 DISCUSSION

We have reported the emission variations of PSR J1752+2359 based on the FAST observation at 1250 MHz. With high sensitivity, FAST provides us with an opportunity to study the single pulses of PSR J1752+2359. We find that this pulsar exhibits two different states: a normal state with continuous pulse emission and an RRAT-like state with sporadic pulse emission. The pulse energies in both states follow log-normal distributions. In the normal state, the average profile has three main

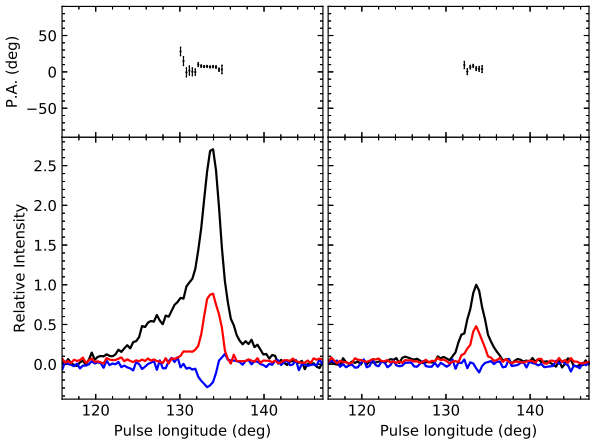

Fig. 6 Similar to Fig. 4, but for the FP (*left*) and LP (*right*).

components, whereas the RRAT-like state has a relatively simple pulse profile with only one main component. The pulse phase offset in the profile peaks between the two states is about $0.^{\circ}35$ at 1250 MHz, while Gajjar et al. (2014) reported a different offset of $0.^{\circ}6 \pm 0.^{\circ}1$ at 327 MHz. This suggested that the offset in the profiles between the two emission states is frequency dependent. Such frequency dependence has been observed in many pulsars, such as PSR B0919+06 (Yu et al. 2019) and PSR J0614+2229 (Rajwade et al. 2016). The polarization properties for the two states are different, and the PA swings for them show different variations. This suggests that the emission geometry may be different in the two states of this pulsar. This is further evidenced by the gradual fall in pulse intensity before the onset of an RRAT-like state which maybe represent a relaxation of the magnetospheric conditions (see Gajjar et al. (2014)). We find that the first and third pulse components disappear prior to the second pulse component towards the end of a normal state, whereas all the three components are present at the beginning of the normal state. The observations with a wider frequency bandwidth (e.g. Parkes ultra-wide-bandwidth receiver, Hobbs et al. 2020) may further reveal the emission properties of this pulsar.

The occurrence of the normal state in PSR J1752+2359 is quasi-periodic with a period of about 568 pulse periods in our observation. Gajjar et al. (2014) also found a similar state-switching period for this pulsar at 325 MHz. The periodical emission variations are seen in many pulsars. By analyzing 123 pulsars at 618/333 MHz, Basu et al. (2016) found that 57 pulsars show periodic characteristics, including 28 phase-modulated drifting pulsars and 29 amplitude-modulated drifting pulsars. They found that the spin-down energy loss rates of the phase-modulated drifting pulsars occupy a narrow range from 10^{30} to 2×10^{32} erg s^{-1}, while that of amplitude-modulated drifting pulsars show a much wider

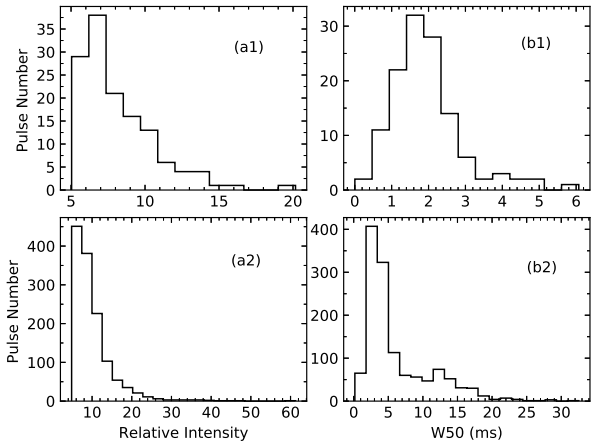

Fig. 7 Plots showing the histograms of peak intensity (a1) and W50 (b1) for pulses in the RRAT-like state, and the corresponding histograms for pulses in the normal state in (a2) and (b2), respectively.

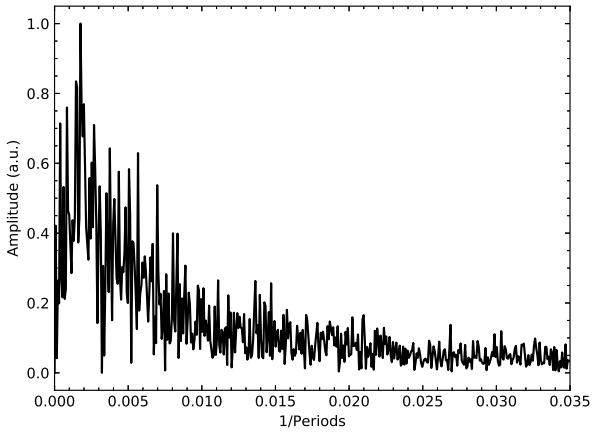

Fig. 8 Result of the fluctuation analysis for PSR J1752+2359, which shows a quasi-periodic feature at 0.00176 cycles per period or 568 pulse periods.

distribution, in the range of 10^{30} to 5×10^{34} erg s^{-1}. The spin-down energy loss rate of PSR J1752+2359 is 3.7×10^{32} erg s^{-1}, which lies in the group of amplitude-modulated drifting pulsars. By analysing a large sample of 70 pulsars that show periodical emission modulations, Basu et al. (2020) suggested that the amplitude-modulated drifting pulsars have a different physical origin compared with the phase-modulated drifting pulsars. Yan et al. (2020) proposed that such amplitude modulation requires emission-state changing in the magnetosphere. The phase-modulated drifting is only seen in cone pulse components, while the amplitude-modulated drifting is seen across the entire profile in both the core and cone pulse components (Basu et al. 2020). The triple form of the mean pulse profile of PSR J1752+2359 suggests that the central and outer components may correspond to the core and cone components, respectively.

The most remarkable feature of PSR J1752+2359 is that it switches between a pulsar-like and an RRAT-like states quasi-periodically. The typical duration of the bursts for RRATs is in the range of 2 to 30 ms and the burst rates are in the range of 0.2 to 436.4 per hour[2]. The duration of pulses in the RRAT-like state of PSR J1752+2359 is several milliseconds and the burst rate is about 109 per hour, which are both consistent with typical RRATs.

The relationship between RRATs and normal pulsars remains a mystery. PSR J1752+2359 is the third pulsar that shows such a switching phenomenon. However, the state-switching period of PSR J1752+2359 is only about 232 s which is much shorter than that of both PSR J0941−39 (Burke-Spolaor & Bailes 2010) and PSR B0826−34 (Esamdin et al. 2012) whose state-cycle periods are about several hours or even much longer. The characteristic ages of these pulsars are around 10^7 yr, which are relatively old in nulling pulsars. This implies that the nulling fraction may increase with characteristic age. By analysing a large sample of nulling pulsars, Wang et al. (2007) also found a similar correlation between the nulling fraction and pulsar age. Timokhin (2010) suggested the freedom in the current density distribution will increase with the aging of a pulsar, which might cause reconfiguration of the pulsar magnetosphere. The FAST pulsar surveys, i.e. CRAFTS (Li et al. 2018) and GPPS (Han et al. 2021), will discovery more pulsars including RRATs, which will help to understand the relationship between pulsars and RRATs.

In summary, we confirmed that PSR J1752+2359 is the third pulsar that oscillates in emission states between being an RRAT and a pulsar. Our polarization observation suggests that the magnetospheric field geometry may be different in the pulsar and RRAT states. We also find that the pulsars showing oscillation between RRAT and pulsar states are relatively old compared to nulling pulsars. Neutron stars that switch between being normal pulsars and RRATs are rare and they are important objects which help us understand the complete evolutionary process of pulsars. In the future, observing more RRATs with FAST will throw more light on their origins.

Acknowledgements We would like to thank A. Esamdin for helpful discussions. This work made use of the data from the FAST (Five-hundred-meter Aperture Spherical radio Telescope). FAST is a Chinese national mega-science facility, built and operated by the National Astronomical Observatories, Chinese Academy of Sciences. This work is supported by the open program of the Key Laboratory of Xinjiang Uygur Autonomous Region (No. 2020D04049), the Joint Research Fund in Astronomy under cooperative agreement between the National Natural Science Foundation of China (NSFC) and the Chinese Academy

[2] http://astro.phys.wvu.edu/rratalog/

of Sciences (CAS) (Nos. U1831102 and U1731238), the NSFC project (Nos. 12041303 and 12041304), the National Key Research and Development Program of China (No. 2016YFA0400804) and the National SKA Program of China (No. 2020SKA0120200). The research is partly supported by the Operation, Maintenance and Upgrading Fund for Astronomical Telescopes and Facility Instruments, budgeted from the Ministry of Finance of China (MOF) and administrated by the CAS.

References

Backer, D. C. 1970, Nature, 228, 42
Bartel, N., Morris, D., Sieber, W., & Hankins, T. H. 1982, ApJ, 258, 776
Basu, R., Mitra, D., & Melikidze, G. I. 2020, ApJ, 889, 133
Basu, R., Mitra, D., Melikidze, G. I., et al. 2016, ApJ, 833, 29
Biggs, J. D. 1992, ApJ, 394, 574
Burke-Spolaor, S., & Bailes, M. 2010, MNRAS, 402, 855
Cui, B. Y., Boyles, J., McLaughlin, M. A., & Palliyaguru, N. 2017, ApJ, 840, 5
Esamdin, A., Abdurixit, D., Manchester, R. N., & Niu, H. B. 2012, ApJL, 759, L3
Feng, Y., Hobbs, G., Li, D., et al. 2021, ApJ, 908, 105
Foster, R. S., Cadwell, B. J., Wolszczan, A., & Anderson, S. B. 1995, ApJ, 454, 826
Gajjar, V., Joshi, B. C., & Wright, G. 2014, MNRAS, 439, 221
Gajjar, V., Yuan, J. P., Yuen, R., et al. 2017, ApJ, 850, 173
Harding, A. K. 2013, Frontiers of Physics, 8, 679
Herfindal, J. L., & Rankin, J. M. 2007, MNRAS, 380, 430
Hewish, A., Bell, S. J., Pilkington, J. D. H., et al. 1968, Nature, 217, 709
Hobbs, G., Manchester, R. N., Dunning, A., et al. 2020, PASA, 37, e012
Hotan, A. W., van Straten, W., & Manchester, R. N. 2004, PASA, 21, 302
Han, J. L., Wang, C., Wang, P. F., et al. 2021, RAA (Research in Astronomy and Astrophysics), 21, 107
Jiang, P., Yue, Y., Gan, H., et al. 2019, Science China Physics, Mechanics, and Astronomy, 62, 959502
Kramer, M., Lyne, A. G., O'Brien, J. T., et al. 2006, Science, 312, 549
Lewandowski, W., Wolszczan, A., Feiler, G., et al. 2004, ApJ, 600, 905
Li, D., Wang, P., Qian, L., et al. 2018, IEEE Microwave Magazine, 19, 112
Lorimer, D. R., Camilo, F., & McLaughlin, M. A. 2013, MNRAS, 434, 347
Lorimer, D. R., & Kramer, M. 2012, Handbook of Pulsar Astronomy (Cambridge, UK: Cambridge Univ. Press)
Lyne, A., & Graham-Smith, F. 2012, Pulsar Astronomy (Cambridge, UK: Cambridge Univ. Press)
Manchester, R. N., Hobbs, G. B., Teoh, A., & Hobbs, M. 2005, AJ, 129, 1993
McLaughlin, M. A., Lyne, A. G., Lorimer, D. R., et al. 2006, Nature, 439, 817
Nan, R. 2008, in SSPIE Conference Series, 7012, Ground-based and Airborne Telescopes II, eds. L. M. Stepp, & R. Gilmozzi, 70121E
Nan, R., Li, D., Jin, C., et al. 2011, International Journal of Modern Physics D, 20, 989
Rajwade, K., Seymour, A., Lorimer, D. R., et al. 2016, MNRAS, 462, 2518
Rankin, J. M., & Wright, G. A. E. 2008, MNRAS, 385, 1923
Ritchings, R. T. 1976, MNRAS, 176, 249
Seymour, A. D., Lorimer, D. R., & Ridley, J. P. 2014, MNRAS, 439, 3951
Sobey, C., Bilous, A. V., Grießmeier, J. M., et al. 2019, MNRAS, 484, 3646
Timokhin, A. N. 2010, MNRAS, 408, L41
van Straten, W., & Bailes, M. 2011, PASA, 28, 1
Wang, N., Manchester, R. N., & Johnston, S. 2007, MNRAS, 377, 1383
Wang, P. F., Han, J. L., Han, L., et al. 2020a, A&A, 644, A73
Wang, S. Q., Wang, J. B., Hobbs, G., et al. 2020b, ApJ, 897, 8
Wang, S. Q., Hobbs, G., Wang, J. B., et al. 2020c, ApJL, 902, L13
Wang, S. Q., Wang, J. B., Wang, N., et al. 2021, ApJ, 913, 67
Yan, W. M., Manchester, R. N., Wang, N., et al. 2020, MNRAS, 491, 4634
Yan, W. M., Manchester, R. N., Wang, N., et al. 2019, MNRAS, 485, 3241
Yu, Y.-Z., Peng, B., Liu, K., et al. 2019, Science China Physics, Mechanics, and Astronomy, 62, 959504
Zhang, L., Li, D., Hobbs, G., et al. 2019, ApJ, 877, 55